Journal of Naval Architecture and Marine Engineering
December, 2019
http://dx.doi.org/10.3329/jname.v16i2.29526 http://www.banglajol.info

EFFECTS OF RADIATION AND CHEMICAL REACTION ON MHD FLOW PAST A VERTICAL PLATE WITH VARIABLE TEMPERATURE AND MASS DIFFUSION

U. S. Rajput[1] and Gaurav Kumar[1*]

[1]Department of Mathematics and Astronomy,University of Lucknow, U.P, India.
*Email: rajputgauravlko@gmail.com

Abstract:

This research investigates the effects of radiation, chemical reaction and porosity of the medium on unsteady flow of a viscous, incompressible and electrically conducting fluid past an exponentially accelerated vertical plate with variable wall temperature and mass diffusion in the presence of transversely applied uniform magnetic field. The plate temperature and the concentration level near the plate increase linearly with time. The fluid model under consideration has been solved by Laplace transform technique. The model contains equations of motion, diffusion equation and equation of energy. To analyze the solution of the model, reasonable sets of the values of the parameters have been considered. The numerical data obtained is discussed with the help of graphs and tables. The numerical values obtained for skin-friction, Sherwood number and Nusselt number have been tabulated. It is found that the velocity of fluid increases when the values of permeability parameter, acceleration parameter and radiation parameter are increased. But trend is reversed with the chemical reaction parameter. It means that the velocity decreases when the chemical reaction parameter is increased.

Keywords: MHD flow, radiation, chemical reaction, variable temperature, mass diffusion, Hall current.

NOMENCLATURE

a^*	absorption constant
b	acceleration parameter
$\bar{b}$	dimensionless acceleration parameter
C	Species concentration in the fluid
$\bar{C}$	The dimensionless concentration
C_P	Specific heat at constant pressure
C_w	Species concentration at the plate
C_∞	The concentration in the fluid
D	Mass diffusion
u,v	Velocity of the fluid in x and z- direction
$\bar{u}$ $\bar{v}$	dimensionless velocity in x and z- direction
T	Temperature of the fluid
K_0	The chemical reaction parameter
M	The magnetic parameter,
m	The Hall parameter($m=\omega_e\tau_e$)
Pr	Prandtl number
R	Radiation parameter
Sc	Schmidt number

Greek symbols

ω_e	Cyclotron frequency of electrons
τ_e	Electron collision time
β	Volumetric coeff. of thermal expansion
β^*	Volumetric coeff. of concentration
υ	The kinematic viscosity
ρ	The fluid density
σ	Electrical conductivity
μ	The magnetic permeability
θ	The dimensionless temperature
μ	The coefficient of viscosity
G_m	Mass Grashof number
G_r	Thermal Grashof number
k	The thermal conductivity
T_∞	The temperature of the fluid
g	Gravity acceleration
T_w	Temperature of the plate
K	Permeability of the medium
t	Time

1813-8535 (Print), 2070-8998 (Online) Received on: Sept., 2016

1. Introduction

The MHD flow problems play important role in different areas of science and technology. These have many applications in industry, for instance, magnetic material processing, glass manufacturing control processes and purification of crude oil. Thermal radiation effects on MHD free convection flow past an impulsively started vertical plate with variable surface temperature and concentration was studied by Suneetha et al. (2008). Further, Suneetha and Reddy (2010) have analyzed radiation and mass transfer effects on MHD free convection flow past a moving vertical cylinder in a porous medium. Radiation effect on chemically reacting MHD boundary layer flow of heat and mass transfer through a porous vertical plate was studied by Ibrahim and Makinde (2011). Mass transfer effects on MHD flows exponentially accelerated isothermal vertical plate in the presence of chemical reaction through porous media was considered by Kumar et al. (2012). Ghachem et al. (2012) have worked on numerical simulation of three-dimensional double diffusive free convection flow and irreversibility studies in a solar distiller. Narayana and Sravanthi (2012) have examined influence of variable permeability on unsteady MHD convection flow past a semi-infinite inclined plate with thermal radiation and chemical reaction. The effects of a longitudinal magnetic field and discrete isoflux heat source size on natural convection inside a tilted sinusoidal corrugated enclosure were investigated by Hussain et al. (2012). MHD boundary layer flow due to exponential stretching surface with radiation and chemical reaction was discussed by Seini and Makinde (2013). Hussein (2013) has considered Finite volume simulation of natural convection in a trapezoidal cavity filled with various fluids and heated from the top wall. Further, Hussein et al. (2013) have established effects of a longitudinal magnetic field and discrete isoflux heat source size on natural convection inside a tilted sinusoidal corrugated enclosure.

Viscous dissipation and radiation effects on MHD natural convection in a square enclosure filled with a porous medium were studied by Ahmed et al. (2014). Etwire et al. (2014) have investigated MHD boundary layer stagnation point flow with radiation and chemical reaction towards a heated shrinking porous surface. Effects of radiation and chemical reaction on MHD free convection flow past a vertical plate in the porous medium was proposed by Mondal et al. (2014). Mâatki et al. (2016) have worked on inclination effects of magnetic field direction in 3D double-diffusive natural convection. Modeling of MHD natural convection in a square enclosure having an adiabatic square shaped body using Lattice Boltzmann Method was presented by Hussein et al. (2016). Adekeye et al. (2017) have analyzed numerical analysis of the effects of selected geometrical parameters and fluid properties on MHD natural convection flow in an inclined elliptic porous enclosure with localized heating. Rajput and Kumar (2017) have worked on radiation effect on MHD flow past an inclined plate with variable temperature and mass diffusion. Further Rajput and Kumar (2017) have examined effects of radiation and porosity of the medium on MHD flow past an inclined plate in the presence of Hall current. Chemical reaction effect on unsteady MHD flow past an impulsively started inclined plate with variable temperature and mass diffusion in the presence of Hall current was presented by Rajput and Kumar (2017). Chemical reaction effect on unsteady MHD flow past an impulsively started oscillating inclined plate with variable temperature and mass diffusion in the presence of Hall current was studied by Rajput and Kumar (2016). Further Rajput and Kumar (2017) have worked on effects of rotation and chemical reaction on MHD flow past an inclined plate with variable wall temperature and mass diffusion. Effect of Hall current on unsteady magneto hydrodynamic flow past an exponentially accelerated inclined plate with variable temperature and mass diffusion was studied by Rajput and Kumar (2018). The objective of the present paper is to study the effects of radiation, chemical reaction and porosity of the medium on flow past an exponentially accelerated vertical plate with variable wall temperature and mass diffusion in the presence of transversely applied uniform magnetic field and Hall current. The model has been solved using the Laplace transforms technique. The effects of various parameters on the velocity, temperature, concentration, skin-friction, Nusselt number and Sherwood number are presented graphically.

2. Mathematical Analysis

The geometrical model of the problem is shown in Fig. 1. The x axis is taken along the vertical plate and z axis is normal to it. Thus the z axis lies in the horizontal plane. The magnetic field B_0 of uniform strength is applied perpendicular to the flow. Initially it has been considered that the plate as well as the fluid is at the same temperature T_∞. The species concentration in the fluid is taken as C_∞. At time t > 0, the plate starts exponentially accelerating in its own plane with velocity $u=u_0 e^{bt}$ and temperature of the plate is raised to T_w. The concentration C_w near the plate is raised linearly with respect to time. The flow model is as follow:

$$\frac{\partial u}{\partial t} = \upsilon \frac{\partial^2 u}{\partial z^2} + g\beta (T - T_\infty) + g\beta^* (C - C_\infty) - \frac{\sigma B_0^2 (u + mv)}{\rho(1+m^2)} - \frac{\upsilon u}{K}, \tag{1}$$

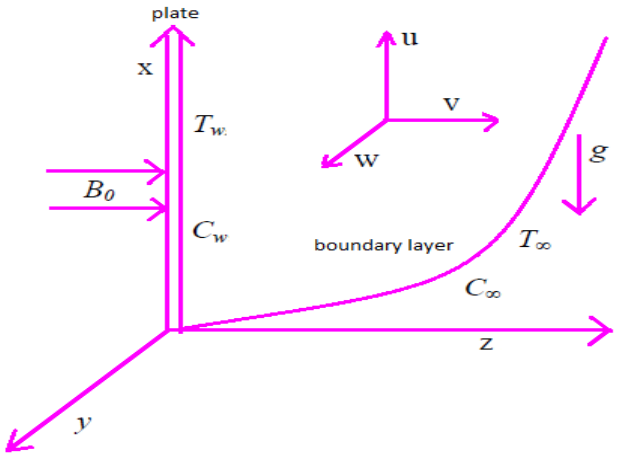

Fig. 1: Physical model

$$\frac{\partial v}{\partial t} = \upsilon \frac{\partial^2 v}{\partial z^2} + \frac{\sigma B_0^2 (mu - v)}{\rho(1+m^2)} - \frac{\upsilon v}{K}, \tag{2}$$

$$\frac{\partial C}{\partial t} = D \frac{\partial^2 C}{\partial z^2} - K_c (C - C_\infty), \tag{3}$$

$$\rho C_p \frac{\partial T}{\partial t} = k \frac{\partial^2 T}{\partial z^2} - \frac{\partial q_r}{\partial z}. \tag{4}$$

The initial and boundary conditions are

$$\left.\begin{array}{l} t \le 0 : u = 0,\ v = 0,\ T = T_\infty,\ C = C_\infty, \text{ for every } z. \\ t > 0 : u = u_0 e^{bt},\ v = 0,\ T = T + (T_w - T_\infty)A,\ C = C_\infty + (C_w - C_\infty)A, \text{ at } z=0. \\ u \to 0,\ v = 0,\ T \to T_\infty,\ C \to C_\infty \text{ as } z \to \infty. \end{array}\right\} \tag{5}$$

The local radiant for the case of an optically thin gray gas is expressed by

$$\frac{\partial q_r}{\partial z} = -4a^* \sigma (T_\infty^4 - T^4), \tag{6}$$

The temperature difference within the flow is considered sufficiently small, hence T^4 can be approximated as the linear function of the temperature. This is accomplished by expanding T^4 in a Taylor series about T_∞ and neglecting higher-order terms, i.e.

$$T^4 \cong 4T_\infty^3 T - 3T_\infty^4. \tag{7}$$

Using equations (6) and (7), equation (4) becomes

$$\rho C_p \frac{\partial T}{\partial t} = k \frac{\partial^2 T}{\partial z^2} - 16a^* \sigma T_\infty^3 (T - T_\infty). \tag{8}$$

The following non-dimensional quantities are introduced to transform equations (1), (2), (3) and (8) into dimensionless form:

$$\left.\begin{aligned} &\bar{z}=\frac{zu_0}{\upsilon},\ \bar{u}=\frac{u}{u_0},\ \bar{v}=\frac{v}{u_0},\quad S_c=\frac{\upsilon}{D},\ K_0=\frac{\upsilon K_c}{u_0^2}\ P_r=\frac{\mu u_0}{k},\bar{b}=\frac{b\upsilon}{u_0^2},\\ &R=\frac{16a^*\upsilon^2\sigma T_\infty^3}{ku_0},\theta=\frac{(T-T_\infty)}{(T_w-T_\infty)},G_r=\frac{g\beta\upsilon(T_w-T_\infty)}{u_0^{\ 3}},\ M=\frac{\sigma B_0^2\upsilon}{\rho u_0^2},\\ &G_m=\frac{g\beta^*\upsilon(C_w-C_\infty)}{u_0^{\ 3}},\mu=\rho\upsilon,\bar{C}=\frac{(C-C_\infty)}{(C_w-C_\infty)},\ \bar{t}=\frac{tu_0^2}{\upsilon}. \end{aligned}\right\} \tag{9}$$

The flow model in dimensionless form is

$$\frac{\partial\bar{u}}{\partial\bar{t}}=\frac{\partial^2\bar{u}}{\partial\bar{z}^2}+G_r\,\theta+G_m\,\bar{C}-\frac{M(\bar{u}+m\bar{v})}{(1+m^2)}-\frac{\bar{u}}{\bar{K}}, \tag{10}$$

$$\frac{\partial\bar{v}}{\partial\bar{t}}=\frac{\partial^2\bar{u}}{\partial\bar{z}^2}+\frac{M(m\bar{u}-\bar{v})}{(1+m^2)}-\frac{\bar{v}}{\bar{K}}, \tag{11}$$

$$\frac{\partial\bar{C}}{\partial\bar{t}}=\frac{1}{S_c}\frac{\partial^2\bar{C}}{\partial\bar{z}^2}-K_0\bar{C}, \tag{12}$$

$$\frac{\partial\theta}{\partial\bar{t}}=\frac{1}{P_r}\frac{\partial^2\theta}{\partial\bar{z}^2}-\frac{R\theta}{P_r}. \tag{13}$$

The corresponding boundary conditions (5) become:

$$\left.\begin{aligned} &\bar{t}\le 0:\bar{u}=0,\ \bar{v}=0,\ \theta=0,\ \bar{C}=0,\quad \text{for every } \bar{z}.\\ &\bar{t}>0:\bar{u}=e^{\bar{b}\bar{t}},\bar{v}=0,\ \theta=\bar{t},\ \bar{C}=\bar{t},\quad \text{at } \bar{z}=0.\\ &\bar{u}\to 0,\ \bar{v}\to 0,\ \theta\to 0,\ \bar{C}\to 0,\quad \text{as } \bar{z}\to\infty. \end{aligned}\right\} \tag{14}$$

Dropping bars in the above equations, we get

$$\frac{\partial u}{\partial t}=\frac{\partial^2 u}{\partial z^2}+G_r\,\theta+G_m\,C-\frac{M(u+mv)}{(1+m^2)}-\frac{u}{K}, \tag{15}$$

$$\frac{\partial v}{\partial t}=\frac{\partial^2 v}{\partial z^2}+\frac{M(mu-v)}{(1+m^2)}-\frac{v}{K}, \tag{16}$$

$$\frac{\partial C}{\partial t}=\frac{1}{S_c}\frac{\partial^2 C}{\partial z^2}-K_0 C, \tag{17}$$

$$\frac{\partial\theta}{\partial t}=\frac{1}{P_r}\frac{\partial^2\theta}{\partial z^2}-\frac{R\theta}{P_r}. \tag{18}$$

The boundary conditions become

$$\left.\begin{aligned} &t\le 0:u=0,v=0,\theta=0,C=0,\quad \text{for every } z.\\ &t>0:u=e^{bt},v=0,\ \theta=t,\ C=t,\quad \text{at z=0.}\\ &u\to 0,\ v\to 0,\ \theta\to 0,\ C\to 0,\quad \text{as } z\to\infty. \end{aligned}\right\} \tag{19}$$

Writing the equations (15) and (16) in combined form (using $q= u + i\,v$)

$$\frac{\partial q}{\partial t}=\frac{\partial^2 q}{\partial z^2}+G_r\,\theta+G_m\,C-qa, \tag{20}$$

$$\frac{\partial C}{\partial t} = \frac{1}{S_c}\frac{\partial^2 C}{\partial z^2} - K_0 C, \tag{21}$$

$$\frac{\partial \theta}{\partial t} = \frac{1}{P_r}\frac{\partial^2 \theta}{\partial z^2} - \frac{R\theta}{P_r}. \tag{22}$$

Finally, the boundary conditions become:

$$\left.\begin{array}{ll} t \le 0 : q = 0, \theta = 0, C = 0, & \text{for every z.} \\ t > 0 : q = e^{bt}, \theta = t, C = t, & \text{at z=0.} \\ q \to 0,\ \theta \to 0,\ C \to 0, & \text{as } z \to \infty. \end{array}\right\} \tag{23}$$

The dimensionless governing equations (20) to (22), subject to the boundary conditions (23), are solved by the usual Laplace transform technique. The solution obtained is as under:

$$q = \frac{1}{2}e^{bt-\sqrt{a+bz}}A_{33} + \frac{G_r}{4(a-R)^2}((\exp(-\sqrt{a}z)(2RtA_1 - 2atA_1 + z\sqrt{a}A_2 + 2A_1(P_r+1)) - \frac{A_2 z}{\sqrt{a}})$$

$$-\frac{2A_5P_r z}{\sqrt{A_{32}}A_{11}}(at - Rt + P_r - 1) + \frac{2A_{28}A_6P_r z}{A_{11}}(P_r - 1) - 2A_{26}A_3(P_r - 1) - \frac{P_r z\sqrt{A_{32}P_r}}{A_{10}\pi\sqrt{R}}(\frac{1}{a} - \frac{1}{R}))$$

$$+\frac{G_m}{4(a-K_0S_c)^2}((\exp(-\sqrt{a}z)(z\sqrt{a}A_2 - 2atA_1 - 2A_1(S_c-1) + 2tA_1K_0S_c) - \frac{z\exp(-\sqrt{a}z)A_2K_0S_c}{\sqrt{a}}$$

$$-2A_{27}A_4(S_c-1)) + \exp(-z\sqrt{S_cK_0})(-\frac{aA_8z\sqrt{S_c}}{\sqrt{K_0}} - 2atA_7 - 2A_7 - 2A_7(S_c-1) + 2tA_7K_0S_c$$

$$+zA_8S_c\sqrt{S_cK_0}) + 2A_{27}A_9(S_c-1))$$

$$\theta = \frac{e^{-\sqrt{R}z}}{4\sqrt{R}}\{erfc[\frac{-2\sqrt{R}t + zP_r}{\sqrt{P_r}t}](2\sqrt{R}t - zR) + e^{2\sqrt{R}z}erfc[\frac{2\sqrt{R}t + zP_r}{\sqrt{P_r}t}](2\sqrt{R}t + zR)\},$$

$$C = \frac{e^{-z\sqrt{S_cK_0}}}{4\sqrt{K_0}}\left\{erfc[\frac{z\sqrt{S_c} - 2t\sqrt{K_0}}{2\sqrt{t}}](-z\sqrt{S_c} + 2t\sqrt{K_0}) + e^{2z\sqrt{S_cK_0}}erfc[\frac{z\sqrt{S_c} + 2t\sqrt{K_0}}{2\sqrt{t}}](z\sqrt{S_c} + 2t\sqrt{K_0})\right\}$$

The expressions for the symbols involved in the above solutions are given in the appendix.

2.1 Skin friction

The dimensionless skin friction at the plate is

$$\left(\frac{dq}{dz}\right)_{z=0} = \tau_x + i\tau_y .$$

The numerical values of τ_x and τ_y, for different parameters are given in Table 1.

2.2 Nusselt number

The dimensionless Nusselt number at the plate is given by

$$Nu = \left(\frac{\partial \theta}{\partial z}\right)_{z=0} = erfc[\frac{\sqrt{Rt}}{\sqrt{tP_r}}](\sqrt{Rt} - \frac{\sqrt{R}}{2}t + \frac{P_r}{4\sqrt{R}}) - erfc[-\frac{\sqrt{Rt}}{\sqrt{tP_r}}](\frac{\sqrt{R}}{2}t + \frac{P_r}{4\sqrt{R}}) - \frac{e^{-\frac{Rt}{P_r}}\sqrt{tP_r}}{\sqrt{\pi}}.$$

The numerical values of *Nu* for different parameters are given in Table 2.

2.3 Sherwood number

The dimensionless Sherwood number at the plate is given by

$$S_h = \left(\frac{\partial C}{\partial z}\right)_{z=0} = erfc[-\sqrt{tK_0}](-\frac{1}{4\sqrt{K_0}}\sqrt{S_c} - \frac{t\sqrt{S_c K_0}}{2}) + \sqrt{S_c}\,erfc[\sqrt{tK_0}](\frac{1}{4\sqrt{K_0}} + t\sqrt{K_0}) - \frac{e^{-tK_0}\sqrt{tS_c K_0}}{\sqrt{\pi K_0}}.$$

The numerical values of S_h for different parameters are given in Table 3.

3. Results and Discussion

The present study is carried out to examine the effects of radiation, chemical reaction and permeability of porous medium on the flow. The behavior of other parameters like magnetic field, Hall current and thermal buoyancy is almost similar the earlier model studied by us (2016). The analytical results are shown graphically in Figs. 2 to 8. The numerical values of skin-friction, Sherwood number and Nusselt number are presented in Table 1, 2 and 3 respectively. From Figs. 4 and 5, it is observed that primary and secondary velocities increase with permeability parameter *(K)*. This result is due to the facts that increase in the value of *(K)* results in reducing the drag force, and hence increasing the fluid velocity. Chemical reaction effect on flow behavior is shown by Figs. 2 and 3. It is seen here that when chemical reaction parameter (K_0) increases, primary and secondary velocities decrease throughout the boundary layer region. Figs. 6 and 7, indicates that effect of radiation (R) in the boundary layer region near the plate tends to accelerate primary and secondary velocities. It is deduced that velocities increase when acceleration parameter b is increased (Figs. 8 and 9). Further, it is observed that the temperature and concentration of the fluid near the plate decrease when radiation and chemical reaction parameters are increased (Figs. 10 and 11).

Skin friction is given in Table 1. The values of τ_x and τ_y increase with the increase in radiation parameter, acceleration parameter and permeability parameter. However, these values decrease with chemical reaction parameter. Sherwood number is given in Table 2. The value of S_h decreases with the increase in the chemical reaction parameter, Schmidt number and time. Nusselt number is given in Table 2. The values of Nu decreases with increase in Prandtl number, radiation parameter and time.

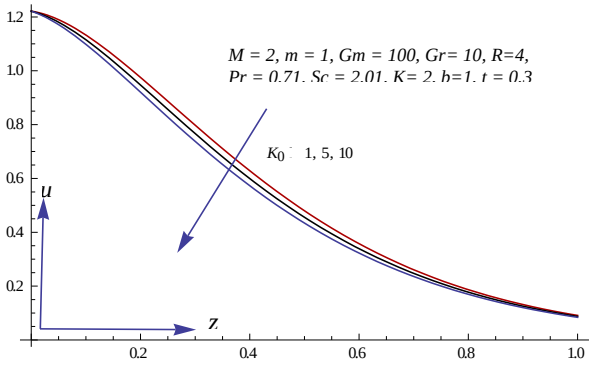

Fig. 2: Velocity u for different values of K_0

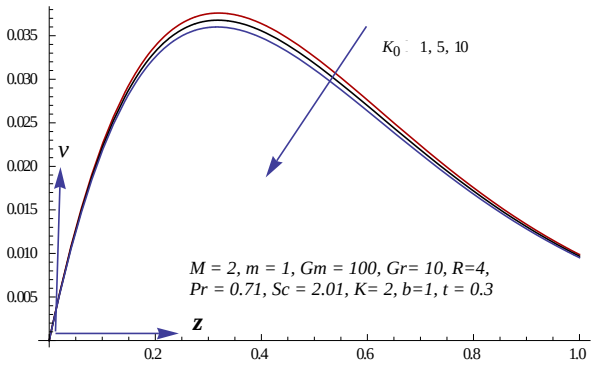

Fig. 3: Velocity v for different values of K_0

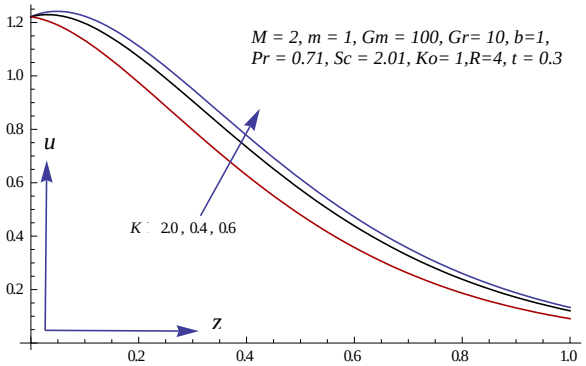

Fig. 4: Velocity u for different values of K

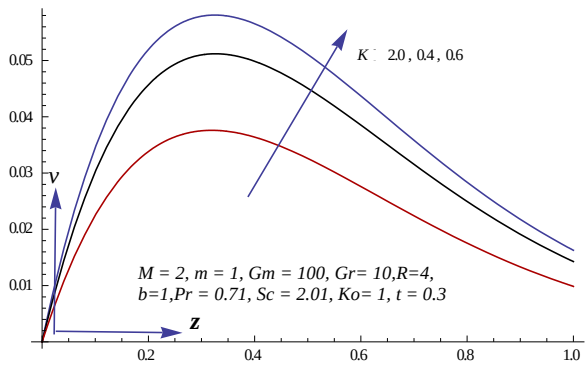

Fig. 5: Velocity v for different values of K

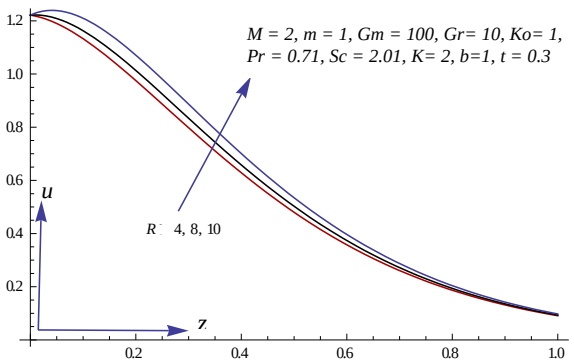

Fig. 6: Velocity u for different values of R

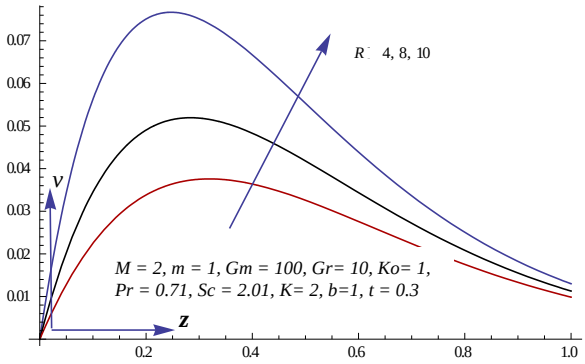

Fig. 7: Velocity v for different values of R

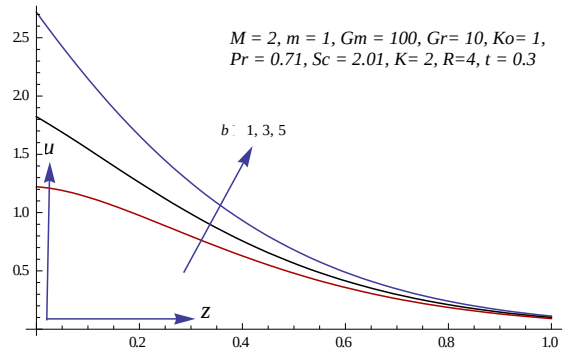

Fig. 8: Velocity u for different values of b

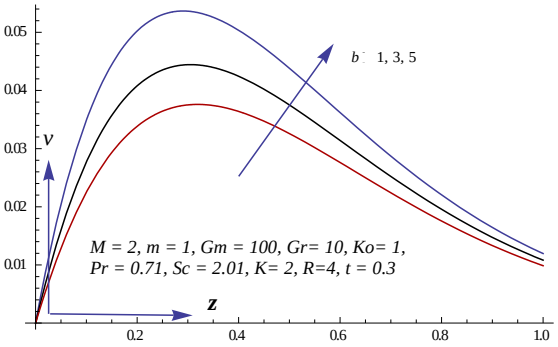

Fig. 9: Velocity v for different values of b

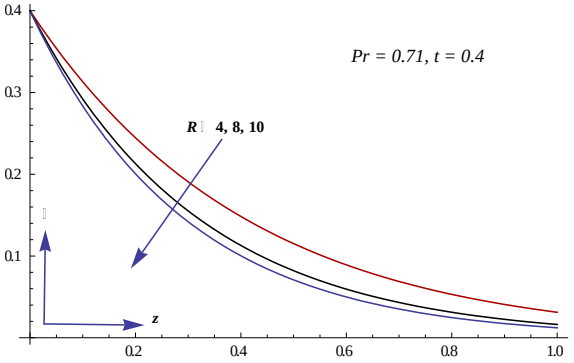

Fig. 10: θ for different values of R

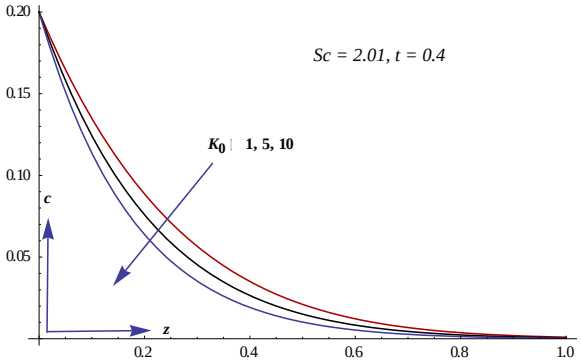

Fig. 11: c for different values of K_0

Table 1: Skin friction for different parameters

M	m	Pr	Sc	Gm	Gr	K	R	K_0	b	t	τ_x	τ_y
2	1	0.71	2.01	100	10	0.2	04	01	1	0.3	088.576	020.553
2	1	0.71	2.01	100	10	0.4	04	01	1	0.3	174.302	066.230
2	1	0.71	2.01	100	10	0.6	04	01	1	0.3	235.485	105.241
2	1	0.71	2.01	100	10	0.2	08	01	1	0.3	309.058	156.476
2	1	0.71	2.01	100	10	0.2	10	01	1	0.3	839.365	583.159
2	1	0.71	2.01	100	10	0.2	04	05	1	0.3	088.117	020.540
2	1	0.71	2.01	100	10	0.2	04	10	1	0.3	087.709	020.528
2	1	0.71	2.01	100	10	0.2	04	01	3	0.3	089.648	020.554
2	1	0.71	2.01	100	10	0.2	04	01	5	0.3	091.597	020.557

Table 2: Sherwood number for different parameters

K_0	Sc	T	S_h
01	2.01	0.2	-0.762200
05	2.01	0.2	-0.933049
10	2.01	0.2	-1.118240
01	3.00	0.2	-0.931175
01	4.00	0.2	-1.075230
01	2.01	0.3	-0.961323
01	2.01	0.4	-1.141570

Table 3: Nusselt number for different parameters

Pr	*R*	*t*	*Nu*
0.71	2	0.4	-0.805273
7.00	2	0.4	-1.959260
0.71	3	0.4	-0.894014
0.71	4	0.4	-0.976083
0.71	2	0.5	-0.950956
0.71	2	0.6	-1.094940

4. Conclusion

In this paper a theoretical analysis has been done to study the unsteady MHD flow through porous medium past an exponentially accelerated vertical plate with variable wall temperature and mass diffusion in the presence of Hall current, radiation and chemical reaction. It has been found that the velocity in the boundary layer increases with the values of permeability parameter, acceleration parameter and radiation parameter. But trend is reversed with chemical reaction parameter. That is velocity decreases when chemical reaction parameter is increased. Skin friction, Sherwood number and Nusselt number are obtained as desired. The results obtained are in agreement with the usual flow. The results obtained will have applications in the research related to the solar physics dealing with the sunspot development, the structure of rotating magnetic stars, cooling of electronic components of a nuclear reactor, bed thermal storage and heat sink in the turbine blades.

References

Adekeye, T., Adegun, I., Okekunle, P., Hussein, A. K., Oyedepo, S., Adetiba, E. and Fayomi, O. (2017): Numerical analysis of the effects of selected geometrical parameters and fluid properties on MHD natural convection flow in an inclined elliptic porous enclosure with localized heating, Heat Transfer-Asian Research, Vol. 46, No.3, pp. 261-293. https://dx.doi.org/10.1002/htj.21211

Ahmed, S., Hussein, A.K., Mohammed, H., Adegun, I., Zhang, X., Kolsi, L., Hasanpour, A. and Sivasankaran, S. (2014): Viscous dissipation and radiation effects on MHD natural convection in a square enclosure filled with a porous medium, Nuclear Engineering and Design, Vol. 266, pp. 34-42.

https://dx.doi.org/10.1016/j.nucengdes.2013.10.016

Etwire C. J., Y. I. Seini, and E. M. Arthur. (2014): MHD boundary layer stagnation point flow with radiation and chemical reaction towards a heated shrinking porous surface, International Journal of Physical Science Vol. 9, No. 14, pp. 320 – 328. https://dx.doi.org/10.5897/IJPS2014.4177

Ghachem, K., Kolsi, L., Mâatki, C., Hussein, A.K. and Borjini, M. (2012): Numerical simulation of three-dimensional double diffusive free convection flow and irreversibility studies in a solar distiller, International Communications in Heat and Mass Transfer, Vol. 39, pp. 869-876.
https://dx.doi.org/10.1016/j.icheatmasstransfer.2012.04.010

Hussein, A.K. (2013): Finite volume simulation of natural convection in a trapezoidal cavity filled with various fluids and heated from the top wall, Universal Journal of Fluid Mechanics, Vol.1, pp. 24-36.

Hussein, A.K., Ashorynejad, H., Sivasankaran, S., Kolsi, L., Shikholeslami, M. and Adegun, I. (2016): Modeling of MHD natural convection in a square enclosure having an adiabatic square shaped body using Lattice Boltzmann Method, Alexandria Engineering Journal, Vol.55, pp. 203-214.

https://dx.doi.org/10.1016/j.aej.2015.12.005

Hussain, S., Hussein, A.K. and Mohammed, R. (2012): Studying the effects of a longitudinal magnetic field and discrete isoflux heat source size on natural convection inside a tilted sinusoidal corrugated enclosure, Computers and Mathematics with Applications, Vol. 64, pp. 476-488.

Hussein, A.K., Hussain, S., Saha, S., Saha, G. and Hasanuzzaman, M. (2013): Effects of a longitudinal magnetic field and discrete isoflux heat source size on natural convection inside a tilted sinusoidal corrugated enclosure, Journal of Basic and Applied Scientific Research , Vol.3, No. 10 , pp. 402-415.

Ibrahim, S. Y. and Makinde, D. (2011): Radiation effect on chemically reacting magnetohydrodynamics (MHD) boundary layer flow of heat and mass transfer through a porous vertical plate, International Journal of Physical Sciences, Vol. 6, No. 6, pp. 1508-1516.

Kumar, J. G, Kishore, P.M. and Ramakrishna, S. (2012): Mass transfer effects on MHD flows exponentially accelerated isothermal vertical plate in the presence of chemical reaction through porous media, Advances in Applied Sciences Research, Vol. 3, No. 4, 2012, pp. 2134-2140.

Mondal, S., Parvin, S. and Ahmmed, S. F. (2014): Effects of radiation and chemical reaction on MHD free convection flow past a vertical plate in the porous medium, American Journal of Engineering Research (AJER) Vol. 3, No. 12, pp. 15-22.

Mâatki, C., Ghachem, K., Kolsi, L., Hussein, A.K., Borjini, M. and Ben Aissia, H. (2016): Inclination effects of magnetic field direction in 3D double-diffusive natural convection, Applied Mathematics and Computation, Vol. 273, pp. 178-189. https://dx.doi.org/10.1016/j.amc.2015.09.043

Narayana P.V.S and Sravanthi S. (2012): Influence of variable permeability on unsteady MHD convection flow past a semi-infinite inclined plate with thermal radiation and chemical reaction" Journal of Energy, Heat and Mass Transfer Vol.34, pp. 143-161.

Rajput U.S. and Kumar G.(2016): Chemical reaction effect on unsteady MHD flow past an impulsively started oscillating inclined plate with variable temperature and mass diffusion in the presence of Hall current, Applied Research Journal, Vol. 2, No. 5, pp. 244-253. https://dx.doi.org/10.11113/mjfas.v12n2.445

Rajput U.S. and Kumar G. (2017): Radiation effect on MHD flow past an inclined plate with variable temperature and mass diffusion. International Journal of Applied Science and Engineering. Vol. 14, No. 3, pp. 171-183.

Rajput U.S. and Kumar G. (2017): Effects of radiation and porosity of the medium on MHD flow past an inclined plate in the presence of Hall current, Computational Methods in Science and Technology, Vol. 23, No. 2, pp. 93–103. https://dx.doi.org/10.12921/cmst.2017.0000003

Rajput U.S. and Kumar G. (2017): Chemical reaction effect on unsteady MHD flow past an impulsively started inclined plate with variable temperature and mass diffusion in the presence of Hall current. Jordan Journal of Mechanical and Industrial Engineering, Vol. 11, No. 1, pp. 041-049.

Rajput U.S. and Kumar G. (2017): Effects of rotation and chemical reaction on MHD flow past an inclined plate with variable wall temperature and mass diffusion , Malaysian Journal of Fundamental and Applied Sciences, Vo l. 13, No. 1, pp. 19- 23. https://dx.doi.org/10.11113/mjfas.v13n1.488

Rajput U.S. and Kumar G. (2018): Effect of Hall current on unsteady magneto hydrodynamic flow past an exponentially accelerated inclined plate with variable temperature and mass diffusion, Matematika, Vol. 34, No. 2, pp. 433-443, https://dx.doi.org/10.11113/matematika.v34.n2.876

Seini Y. I. and Makinde O. D.(2013): MHD boundary layer flow due to exponential stretching surface with radiation and chemical reaction, Mathematical Problems in Engineering, Vol. 2013, pp. 1-7 https://dx.doi.org/10.1155/2013/163614

Suneetha S. and Reddy N. B.(2010): Radiation and mass transfer effects on MHD free convection flow past a moving vertical cylinder in a porous medium, Journal of Naval Architecture and Marine Engineering, Vol. 7, No. 1, pp.1-10. https://dx.doi.org/10.3329/jname.v7i1.2901

Suneetha S., Reddy N. B and Prasad V. R.(2008): Thermal radiation effects on MHD free convection flow past an impulsively started vertical plate with variable surface temperature and concentration, Journal of Naval Architecture and Marine Engineering, Vol. 5, No. 2, pp. 57-70. https://dx.doi.org/10.3329/jname.v5i2.2695

Appendix:

$$A=\frac{u_0^2 t}{\upsilon},\ a=\frac{M(1-im)}{1+m^2}+\frac{1}{K},\ A_1=(1+A_{12}+e^{2\sqrt{az}}(1-A_{13})),\ A_2=(1+A_{12}-e^{2\sqrt{az}}(1-A_{13})),$$

$$A_3=(A_{14}-1+A_{29}(A_{15}-1)),\ A_4=(A_{16}-1+A_{30}(A_{17}-1)),\ A_5=(A_{18}-1+A_{33}(A_{19}-1)),$$

$$A_6=(A_{20}-1+A_{31}(A_{21}-1)),\ A_7=(e^{2z\sqrt{K_0 S_c}}(A_{23}-1)-A_{22}-1)),\ A_8=(e^{2z\sqrt{K_0 S_c}}(A_{23}-1)+A_{22}+1)),$$

$$A_9=(A_{30}(A_{25}-1)-A_{24}-1),\ A_{10}=(1-A_{18}+A_{32}(A_{19}-1)),\ A_{11}=Abs[z]Abs[P_r],$$

$$A_{12}=erf[\frac{1}{2\sqrt{t}}(2\sqrt{a}t-z)],\ A_{13}=erf[\frac{1}{2\sqrt{t}}(2\sqrt{a}t+z)],\ A_{14}=erf[\frac{1}{2\sqrt{t}}(z-2t\sqrt{\frac{aP_r-R}{P_r-1}})],$$

$$A_{15}=erf[\frac{1}{2\sqrt{t}}(z+2t\sqrt{\frac{aP_r-R}{P_r-1}})],\ A_{16}=erf[\frac{1}{2\sqrt{t}}(z-2t\sqrt{\frac{(a-K_0)S_c}{S_c-1}})],\ A_{17}=erf[\frac{1}{2\sqrt{t}}(z+2t\sqrt{\frac{(a-K_0)S_c}{S_c-1}})],$$

$$A_{18}=erf[\frac{A_{11}}{2\sqrt{t}}-\sqrt{\frac{tR}{P_r}}],\ A_{19}=erf[\frac{A_{11}}{2\sqrt{t}}+\sqrt{\frac{tR}{P_r}}],\ A_{20}=erf[\frac{A_{11}}{2\sqrt{t}}-\sqrt{\frac{(R-aP_r)t}{P_r-P_r^2}})],$$

$$A_{21}=erf[\frac{A_{11}}{2\sqrt{t}}+\sqrt{\frac{(R-aP_r)t}{P_r-P_r^2}})],\ A_{22}=erf[\frac{1}{2\sqrt{t}}(2t\sqrt{K_0}-z\sqrt{S_c})],\ A_{23}=erf[\frac{1}{2\sqrt{t}}(2t\sqrt{K_0}+z\sqrt{S_c})],$$

$$A_{24}=erf[\frac{1}{2\sqrt{t}}(2t\sqrt{\frac{(a-K_0)S_c}{S_c-1}}-z\sqrt{S_c})],\ A_{25}=erf[\frac{1}{2\sqrt{t}}(2t\sqrt{\frac{(a-K_0)S_c}{S_c-1}}+z\sqrt{S_c})],$$

$$A_{26}=\exp(\frac{at}{P_r-1}-\frac{Rt}{P_r-1}-z\sqrt{\frac{aP_r-R}{P_r-1}}),\ A_{27}=\exp(\frac{at}{S_c-1}-\frac{tS_cK_0}{S_c-1}-z\sqrt{\frac{(a-K_0)S_c}{S_c-1}}),$$

$$A_{28}=\frac{1}{A_{31}}\exp(\frac{at}{P_r-1}-\frac{Rt}{P_r-1}),\ A_{29}=\exp(2z\sqrt{\frac{-R+aP_r}{P_r-1}}),\ A_{30}=\exp(2z\sqrt{\frac{(a-K_0)S_c}{S_c-1}}),$$

$$A_{31}=\exp(2Abs[z]\sqrt{\frac{P_r(aP_r-R)}{P_r-1}}),\ A_{32}=\exp(2Abs[z]\sqrt{P_rR}),$$

$$A_{33}=1+A_{34}+e^{2\sqrt{a+b}z}A_{35},\ A_{34}=erf[\frac{2\sqrt{a+b}t-z}{2\sqrt{t}}],\ A_{35}=erfc[\frac{2\sqrt{a+b}t+z}{2\sqrt{t}}],$$